NANOSTRUCTURES IN THE QUANTUM HALL REGIME

Eero Tölö

Aalto University *School of Science and Technology*
Faculty of Information and Natural Sciences
Department of Applied Physics
Espoo, Finland

Dissertation for the degree of Doctor of Science in Technology to be presented with due permission of the Faculty of Information and Natural Sciences for public examination and debate in Auditorium K at Aalto University School of Science and Technology (Espoo, Finland) on the 20th August, 2010, at 12 o'clock.

Dissertations of Department of Applied Physics
Aalto University *School of Science and Technology*
ISSN 1797-9595 (print)
ISSN 1797-9609 (online)

Dissertation 162 (2010):
Eero Tölö: Nanostructures in the quantum Hall regime

Opponent:
Prof. Arkadiusz Wójs, University of Cambridge, United Kingdom

Pre-examiners:
Prof. Robert Van Leeuwen, University of Jyväskylä, Finland
Prof. Igor Zozoulenko, Linköping University, Sweden

ISBN 978-952-60-3277-1 (print)
ISBN 978-952-60-3278-8 (online)

Multiprint Oy
Espoo 2010

Aalto University

ABSTRACT OF DOCTORAL DISSERTATION	AALTO UNIVERSITY SCHOOL OF SCIENCE AND TECHNOLOGY P.O. BOX 11000, FI-00076 AALTO http://www.aalto.fi

Author Eero Tölö

Name of the dissertation
Nanostructures in the quantum Hall regime

Manuscript submitted April 14, 2010	Manuscript revised -
Date of the defence August 20, 2010	
☐ Monograph	☑ Article dissertation (summary + original articles)

Faculty	Faculty of Information and Natural Sciences
Department	Department of Applied Physics
Field of research	Theoretical Condensed Matter Physics
Opponent(s)	Professor Arkadiusz Wójs
Supervisor	Professor Risto Nieminen
Instructor	Doctor Ari Harju

Abstract

The quantum Hall effect observed in a two-dimensional electron gas exposed to a perpendicular magnetic field is one of the most important modern discoveries in condensed matter physics. Advances in technology have allowed both experimental and computer-based theoretical study of miniature-size counterparts of conventional quantum Hall devices. Due to their versatile tunable electronic and magnetic properties, these systems show great promise for future technological applications.

This work investigates two-dimensional semiconductor quantum dots and extended quantum rings in the quantum Hall regime. Besides being interesting on purely theoretical grounds as experimentally reachable extreme quantum-mechanical interacting many-body systems, the systems considered have major applicational interest in the realm of quantum information processing.

Our emphasis lies in the strongly correlated regime where the enhanced electron-electron interactions lead to a computationally hard problem. For the systems with a few electrons, we employ the in principle exact configuration interaction method, which allows accurate study of the effects of the confinement potential and the effective form of the electron-electron interaction. Larger systems are modeled by Monte Carlo and density functional based methods. Moreover, we develop a computational method based on the reduced density-matrix functional theory to study the physics at the strongly correlated fractional quantum Hall regime with large particle numbers.

The main results are related to the interplay of electron correlation and magnetism as well as the effects of tuning the electron correlation through sample engineering. The results on magnetism may find applications in future spintronics devices and spin qubits. Meanwhile, the results on electron correlation are relevant for the attempts to utilize fractional quantum Hall states in topologically protected quantum computing.

Keywords quantum Hall effect, quantum dot, quantum ring	
ISBN (printed) 978-952-60-3277-1	ISSN (printed) 1797-9595
ISBN (pdf) 978-952-60-3278-8	ISSN (pdf) 1797-9609
Language English	Number of pages 124
Publisher Department of Applied Physics, Aalto University	
Print distribution Department of Applied Physics, Aalto University	
☑ The dissertation can be read at http://lib.tkk.fi/Diss/2010/isbn9789526032788/	

Aalto-yliopisto

VÄITÖSKIRJAN TIIVISTELMÄ	AALTO-YLIOPISTO TEKNILLINEN KORKEAKOULU PL 11000, 00076 AALTO http://www.aalto.fi

Tekijä Eero Tölö

Väitöskirjan nimi

Nanorakenteet kvantti-Hall-alueella

Käsikirjoituksen päivämäärä 14.04.2010	Korjatun käsikirjoituksen päivämäärä -
Väitöstilaisuuden ajankohta 20.08.2010	
☐ Monografia	☑ Yhdistelmäväitöskirja (yhteenveto + erillisartikkelit)

Tiedekunta	Informaatio- ja luonnontieteiden tiedekunta
Laitos	Teknillisen fysiikan laitos
Tutkimusala	Teoreettinen tiiviin aineen fysiikka
Vastaväittäjä(t)	Professori Arkadiusz Wójs
Työn valvoja	Professori Risto Nieminen
Työn ohjaaja	Tohtori Ari Harju

Tiivistelmä

Kohtisuoralle magneettikentälle altistetussa elektronikaasussa havaittava kvantti-Hall-ilmiö on modernin tiiviin aineen fysiikan merkittävimpiä löytöjä. Tekniikan kehityksen ansiosta voidaan nykyisin tutkia pienoiskokoisia kvantti-Hall-systeemejä sekä kokeellisesti että teoreettisin laskennallisin keinoin. Monipuolisten säätyvien elektronisten ja magneettisten ominaisuuksiensa vuoksi näille voi löytyä käyttöä huipputeknologian sovelluksissa.

Väitöskirjassa tutkitaan kaksiulotteisia puolijohdekvanttipisteitä ja -renkaita kvantti-Hall-ilmiön vaikutusalueella. Tutkittavat kohteet ovat kiinnostavia paitsi teoreettiselta kannalta kokeelliset tutkimukset mahdollistavina äärimmäisen kvanttimekaanisina vuorovaikuttavina monen kappaleen systeemeinä myös soveltavalta kannalta kvantti-informaatioteknologian piirissä.

Tutkimuksen pääpaino on voimakkaan korrelaation alueella, jossa tehostunut elektronien välinen vuorovaikutus johtaa laskennallisesti vaikeaan ongelmaan. Mallinnamme elektronilukumäärältään pieniä systeemejä käytännössä tarkalla konfiguraatiovuorovaikutusmenetelmällä, joka mahdollistaa kvanttipisteen sähköisen koossapitopotentiaalin ja elektronien välisen vuorovaikutuksen muodon vaikutusten tutkimisen. Suurempia systeemejä mallinnamme Monte Carlo -tekniikkaan ja funktionaaleihin perustuvilla menetelmillä. Väitöskirjassa myös kehitetään redusoidun tiheysmatriisin käyttöön perustuva laskennallinen menetelmä voimakkaasti korreloidun murtolukuisen kvantti-Hall-alueen tutkimiseen suuremmilla elektroniluvuilla.

Keskeiset tulokset liittyvät elektronikorrelaation ja magnetismin vuorovaikutteisuuteen sekä näytteen ominaisuuksien säätelyn elektronikorrelaatioon aiheuttamaan vaikutukseen. Magnetismia koskevat tulokset voivat löytää sovellutuksia spintroniikasta ja spinkubiteista. Elektronikorrelaatioista saadut tulokset ovat puolestaan olennaisia murtolukuisten kvantti-Hall-tilojen hyödyntämisessä topologisesti virhesuojatussa kvanttilaskennassa.

Asiasanat kvantti-Hall-ilmiö, kvanttipiste, kvanttirengas

ISBN (painettu) 978-952-60-3277-1	ISSN (painettu) 1797-9595
ISBN (pdf) 978-952-60-3278-8	ISSN (pdf) 1797-9609
Kieli englanti	Sivumäärä 124

Julkaisija Teknillisen fysiikan laitos, Aalto-yliopisto

Painetun väitöskirjan jakelu Teknillisen fysiikan laitos, Aalto-yliopisto

☑ Luettavissa verkossa osoitteessa http://lib.tkk.fi/Diss/2010/isbn9789526032788/

Acknowledgements

The work presented in the thesis has been done in the Quantum Many-body Physics group, a hither part of the Helsinki Institute of Physics in the Aalto University School of Science and Technology (former Helsinki University of Technology). Particularly praiseworthy is the notable financial support offered by the Vilho, Yrjö, and Kalle Väisälä Foundation that very kindly granted scholarships for both years of my graduate studies.

Ywis, there are folks who I will thank herein: My supervisor professor Risto Nieminen for occasional words of advice during the years and careful reading of the final manuscript. My undoubtedly helpful instructor Ari Harju for guidance and various spare parts.

I am grateful to my coauthors Gustav Bårdsen, Yvette Hancock, Esa Räsänen, Henri Saarikoski, and Juha Suorsa for their contribution and fruitful collaboration. Similarly, it has been a pleasure to share the office with Mikko Ervasti, Jaakko Nissinen, Jani Särkkä, and Christian Webb over the years. Thanks to Esko Keski-Vakkuri, Timo Lähde, and others for interesting discussions. Finally, I thank my friends and family for spare time comforts.

Espoo, June 21, 2010

Eero Tölö

Contents

List of publications

This thesis consists of an overview and the following publications:

I E. Tölö, J. Suorsa, and A. Harju,
Two interacting electrons in a square quantum dot,
Physica E **40**, 1038 (2008).

II Y. Hancock, J. Suorsa, E. Tölö, and A. Harju,
Fractional periodicity and magnetism of extended quantum rings,
Physical Review B **77**, 155103 (2008).

III H. Saarikoski, E. Tölö, A. Harju, and E. Räsänen,
Pfaffian and fragmented states at $\nu = \frac{5}{2}$ in quantum Hall droplets,
Physical Review B **78**, 195321 (2008).

IV E. Tölö and A. Harju,
Effects of thickness in quantum dots in strong magnetic fields,
Physical Review B **79**, 075301 (2009).

V E. Tölö and A. Harju,
Quantum Hall droplet laterally coupled to a quantum ring,
Physical Review B **80**, 045303 (2009).

VI G. Bårdsen, E. Tölö, and A. Harju,
Magnetism in tunable quantum rings,
Physical Review B **80**, 205308 (2009).

VII E. Tölö and A. Harju,
Optimal confinement potential in quantum Hall droplets,
Physica E **42**, 1050 (2010).

VIII E. Tölö and A. Harju,
Reduced density-matrix functional theory in quantum Hall systems,
Physical Review B **81**, 075321 (2010).

The author has had an active role in all the research reported in this thesis. He has been one of the major contributors to the development of the ED computer programs and developed the RDMFT programs employed to calculate the results presented in Publications **I**-**VIII**. The author has designed the work and performed the calculations reported in Publications **I**, **IV**-**V**, and **VII**-**VIII**, and has written, apart from **I**, the main drafts of those papers. He has contributed to the programming, the computation of the results, and the writing process of Publications **II**, **III**, and **VI**.

Chapter 1

Introduction

In this thesis, the interest is focused on two-dimensional electron systems exposed to a perpendicular magnetic field. Planar electrons in magnetic field made it big with the experimental discovery of the integer and fractional quantum Hall effect in the early 80s, the observation that the transverse conductance σ_{xy} attains discrete values at integer, or more generally certain rational numbers, ν in the fundamental units e^2/h (here e is the elementary charge and h is the Planck's constant). While allowing for a practical resistance standard used now worldwide, equally important are the conceptual discoveries resulting from the process of understanding the phenomenon. Among these are the quasiparticles with fractional charge and statistics, composite particles of charge and flux, and topological order, which separates different phases in the absence of a symmetry breaking.

Besides such developments in the purely theoretical side, there are two other notable modern trends, on which this work is based. The first is more or less methodological as it influences the very way we do our work – the computers and their ever more growing capacity to solve large problems. The second is the continuous development in the experimentation and fabrication of nanoscopic samples and devices. With highly sophisticated techniques, it is nowadays possible to trap a controllable number of electrons to nanostructures of various shape and size. These devices are of great potential for future technological applications.

That being said, the present work can be summarized as a triple play of quantum Hall theory, computational physics, and the models motivated by the experimental nanosystems: quantum dots and quantum rings. The remainder of this introductory part aims to provide the reader with

the necessary concepts and ideas that lie behind and motivate the work presented in the enclosed publications. Chapter 2 reviews selected physical concepts and discoveries with an eye to how they relate to author's own work while Chapter 3 presents the computational methods used in the studies. The final Chapter 4 briefly summarizes the content of the work.

Chapter 2

Physical concepts

In what follows, we review some basic physics of two-dimensional electron systems in a magnetic field. The aim is to provide a sufficient amount of information in a convenient form such that the reader can comfortably proceed to study the enclosed publications. Unnecessary technical details are left in the referenced original papers as well as the many review articles and books that have been written.

First, the low-dimensional nanostructures that arise in the context of semiconductor heterostructures are introduced (Section 2.1), after which a model for such systems is presented (Section 2.2). The solutions of the model lead to phase vortices and composite particles (Section 2.3). Some real world experimental consequences are subsequently demonstrated in the context of the quantum Hall effect (Sections 2.4 and 2.5). Finally, remarks are made about the one-dimensional edge of the system (Section 2.6), which is an important topic both in theory and experiments.

2.1 Low-dimensional semiconductor nanostructures

Although materials are three dimensional, there are many important physical systems where the motion of electrons (or holes) is restricted to effectively two spatial dimensions. Perhaps the most common is the two-dimensional electron gas (2DEG) found at the semiconductor-insulator or semiconductor-semiconductor interface in field-effect transistors and similar de-

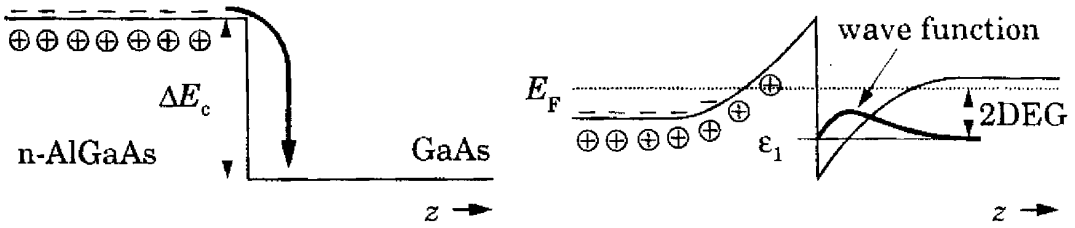

Figure 2.1: Formation of two-dimensional electron gas in modulation doped $Al_xGa_{1-x}As$-GaAs semiconductor heterojunction. Adapted from Ref. [4] by Davies.

vices. Other much studied examples are electrons confined to move along the surface of a material (e.g. the first studied 2DEG on liquid Helium) or in a single sheet of graphene, the two-dimensional honeycomb crystal lattice of carbon atoms that has gained much attention in recent years.

Historically, 1960s was a decade of intense research efforts to confine electrons to thin layers primarily in metals, superconductors, and metal-oxide-semiconductor devices [1, 2]. Relevant to this work are the 2D electron systems confined to the interface of a semiconductor-semiconductor heterojunction discovered in the early 1970s. The scientific breakthroughs back then opened the field of two-dimensional electron systems, the subject of a famous conference series EP2DS [3] (Publications **I** and **VII** are proceedings thereof). Figure 2.1 illustrates the formation of 2DEG in the case of a modulation doped $Al_xGa_{1-x}As$-GaAs junction, which is perhaps the best-studied junction of this type in the literature [4].

To elucidate the matter, $Al_xGa_{1-x}As$ (abbreviated AlGaAs not to be understood as a chemical formula) is a semiconductor alloy composed of AlAs and GaAs, which has slightly larger band gap than GaAs so that the conduction band lies higher (Fig. 2.1 left). When the two materials are connected, the Fermi levels (chemical potentials) of the two sides are matched, the energy bands bend (Fig. 2.1 right), and electrons from the dopant atoms in AlGaAs are transferred to GaAs forming a dipolar potential well and a 2DEG just behind the interface. Modulation doping means that the donors are placed a small distance away from the interface so that they do not scatter electrons of the 2DEG. Moreover, because the alloy structure of AlGaAs is similar to the crystal structure of GaAs (about the same lattice constant), they can be joined without strain to form a high quality interface with little impurity scattering. The samples are usually grown

by molecular-beam epitaxy, which, combined with the small effective mass[1] of electrons in GaAs, allows very high mobilities[2] of charge carriers in the 2DEG at low temperature. The mean free path of an electron may then be as long as 0.1 mm [5]. However, it must be stressed that these numbers refer to systems at very low temperature ($k_{\mathrm{B}}T \ll 1$ meV meaning $T \ll 10$ K), which are thus presently interesting primarily for the purposes of fundamental physics. Other commercially more promising low-dimensional materials with high mobilities even at the room temperature include carbon nanotubes and graphene.

Although the thickness of the 2DEG, the width of the electron density in the direction perpendicular to the interface, typically corresponds to several crystalline monolayers, the excitations in the perpendicular direction (z-direction) have relatively high energy, and thus the motion of electrons is effectively two-dimensional. This owes particularly to the small effective mass and thus the large de Broglie wavelength of electrons in semiconductors ($\lambda = h/m^*v$). Even though there are no low-energy degrees of freedom in the z-direction, the thickness of the ground-state wave function affects the effective Coulomb interaction between the electrons in the 2DEG obtained as the z-dependence is traced out. The effective interaction can be approximated as

$$V_{\mathrm{eff}}(r) = \frac{e^2}{4\pi\epsilon\sqrt{r^2 + d_{\mathrm{t}}^2}} \tag{2.1.1}$$

with parameter d_{t} comparable to the thickness of the electron density, and ϵ the static dielectric constant of the semiconductor. Similarly, it is possible that the interaction between the electrons is screened due to a near-by metallic layer or other traced out degrees of freedom (such as lower Landau levels when working with a model projected to higher Landau levels (see Sec. 2.2)). One possible approximation to the effective interaction in such case has the form

$$V_{\mathrm{eff}}(r) = \frac{e^2 \exp(-(r/d_{\mathrm{s}})^2)}{4\pi\epsilon r} \,, \tag{2.1.2}$$

where d_{s} gives typical length scale of the screening.

[1] The effective mass of the charge carriers in GaAs is $m^* \approx 0.067 m_e$. This follows from the approximately valid parabolic dispersion relation $E(k) \approx E_{\mathrm{c}} + (\hbar k)^2/2m^*$ in the low-energy sector of the GaAs conduction band $E(k) - E_{\mathrm{c}} \lesssim 100$ meV. Here k is the wave vector and E_{c} is the minimum energy of the conduction band located at the Γ point in k-space. The small effective mass is responsible for the enhanced quantum effects (large quantum fluctuations at relatively large length scales) and the strong influence of electromagnetic interactions leading to rich physics in semiconductor nanostructures.

[2] Mobility, $\mu = e\tau/m^*$ where τ is the relaxation-time to the scattering, is the proportionality constant relating the drift-velocity of charge carriers to the applied electric field $v_{\mathrm{d}} = \mu E$.

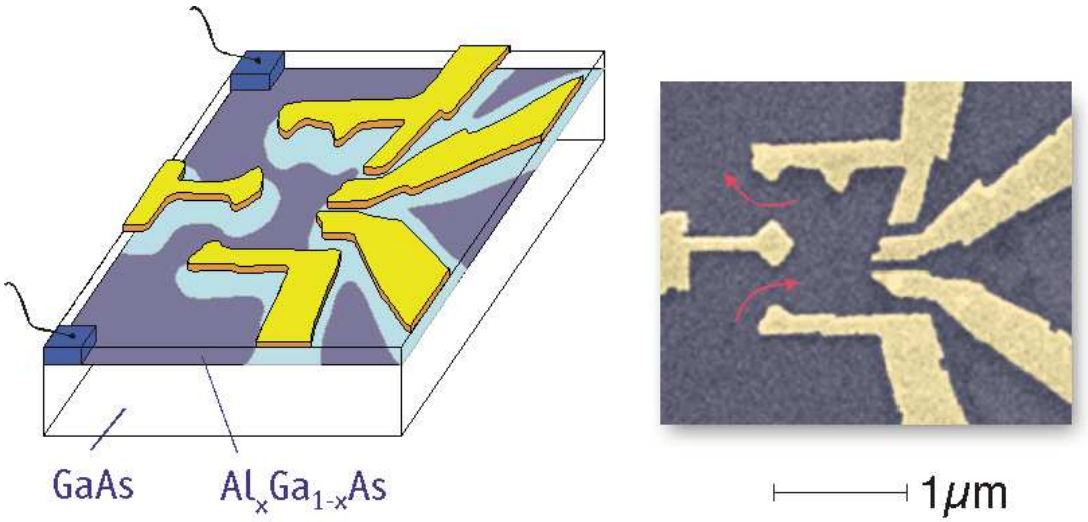

Figure 2.2: A lateral quantum dot device. The shape and transport through the two-dimensional quantum dot formed in the $Al_xGa_{1-x}As$-GaAs heterojunction is controlled by altering the voltages of the metal gates lying on top of the AlGaAs layer. Adapted from Ref. [6] by Kouwenhoven and Marcus.

With the development of advanced technology, it has become possible to further confine a controllable number of electrons to a narrow strip (quantum wire), nanoscale area or volume (quantum dot [7]), narrow ring (quantum ring), or almost any other imaginable minuscule structure. Figure 2.2 shows a lateral quantum dot device, an AlGaAs-GaAs heterostructure with additional metal electrodes (gates) patterned on top of the AlGaAs layer using electron-beam lithography. Applying gate voltages, a charge depletion of tunable form can be inflicted around a quantum dot forming in the 2DEG at the heterostructure interface. Typically, the thickness of such a quantum dot is small compared to the size of the dot in the planar directions, and the dot can be treated as a quasi-two-dimensional. Alternative to lateral quantum dots, vertical quantum dots are created by etching away part of heterostructure's layers leaving a vertical pillar whose physical edges mark the edges of the quantum dot. Confinement of this type has the disadvantage of edge defects that are not present in the lateral devices. However, the first quantum dots created in 1986 in research laboratories of Texas Instruments Inc. [8] were of this type and the technique is still largely applied. Quasi-one-dimensional quantum rings can be created, for example, by forcing the charge away from the central region of the quantum dot.

Besides the two-dimensional quantum dots described above, there are also three-dimensional

quantum "dots" or clusters. Quantum dots in general have various possible applications including quantum information processing (qubits [9]), light-emitting devices (e.g. LEDs [10], lasers [11]), photovoltaic devices (e.g. solar cells [12]) and even in medical sciences (e.g. markers or dyes [13]). Among these, the qubit applications are closest in spirit to the quantum dots studied in this work. However, our theoretical study of quantum dots with many electrons is also related to the applications of quantum Hall devices (see the end of Secs. 2.4 and 2.5). Additionally, it might be possible to use small quantum Hall systems to realize quantum dot qubits that reduce the decoherence problem.

2.2 2D electrons in magnetic field

It turns out to be worth the effort to apply a magnetic field normal to the plane of the nanostructures presented previously. The general form of the quasi-two-dimensional effective Hamiltonian used to model the electrons confined to a semiconductor nanostructure with parabolic energy-momentum dispersion relation reads

$$H = \sum_{i=1}^{N} \left[\frac{(\mathbf{p}_i + e\mathbf{A}(\mathbf{r}_i))^2}{2m^*} + V_{\text{ext}}(\mathbf{r}_i) + g^*\mu_B \mathbf{B} \cdot \hat{\mathbf{S}}_i/\hbar \right] + \sum_{i<j}^{N} V_{\text{eff}}(r_{ij}) \,, \tag{2.2.1}$$

where $\mathbf{r}_i \in \mathbb{R}^2$, N is the number of electrons confined by the lateral external potential V_{ext} and interacting through effective interaction V_{eff}, $\mathbf{A}$ is the vector potential of the external magnetic field $\mathbf{B}$ that pierces the sample plane, $\hat{\mathbf{S}} = \frac{\hbar}{2}(\sigma_x, \sigma_y, \sigma_z)$ with the Pauli matrices σ_i, and $\mu_B = e\hbar/2m_e$ is the Bohr magneton. The relevant material parameters in GaAs are the effective electron mass $m^* = 0.067m_e$, the effective electron gyromagnetic ratio $g^* = -0.44$, and the dielectric permittivity $\epsilon = 12.7\epsilon_0$.

By choosing an appropriate confinement potential V_{ext}, the above Hamiltonian is used to model anything from coupled extended quantum rings and quantum dots to macroscopic quantum Hall samples. However, because of the electron-electron interaction V_{eff}, the energy states of the system can not be calculated analytically but are obtained by numerical techniques (see Chapter 3). In Publications **I** and **II**, V_{ext} is of the square (**I**, [14]) or circular (**II**) hard-wall form leading to a square or circular quantum dot. For the purposes of this overview, we concentrate

on the more commonly used parabolic confinement potential

$$V_{\text{ext}}(r) = \frac{1}{2} m^* \omega_0^2 r^2 \,, \tag{2.2.2}$$

which has the advantage of simple form of the single-particle spectrum at arbitrary strength of the magnetic field. Furthermore, the rotational symmetry increases the efficiency of numerical implementations and thus allows an exact numerical treatment of larger electron numbers.

In the symmetric gauge $\mathbf{A}(\mathbf{r}) = (y, -x)B/2$, the single-particle energy states called Fock-Darwin states are written as [15, 16]

$$\begin{aligned} \psi_n^m(z) =& \sqrt{\frac{n!}{\pi(m+n)!}} z^m L_n^m(z\bar{z}) \exp\left(-z\bar{z}/2\right),\ m \geqslant -n,\ n \geqslant 0 \,, \\ E_n^m =& (2n+1)\hbar\omega + m\left(\hbar\omega - \frac{\hbar\omega_c}{2}\right) + g^*\mu_B B s_z \,, \end{aligned} \tag{2.2.3}$$

where the complex coordinate $z = (x + iy)/l$ and L_n^m is a generalized Laguerre polynomial

$$L_n^m(x) = \sum_{k=0}^{n} \frac{(-x)^k}{k!} \binom{m+n}{n-k} \,, \tag{2.2.4}$$

which reduces to 1 and $-x + m + 1$ for n equal to 0 and 1, respectively. The oscillator length l is defined as $l = \sqrt{\hbar/m^*\omega}$ where the angular oscillator frequency ω depends on the magnetic field and the strength of the parabolic confinement through $\omega = \sqrt{\omega_0^2 + (eB/2m)^2} = \sqrt{\omega_0^2 + (\omega_c/2)^2}$ with the cyclotron frequency ω_c.[3]

Figure 2.3(a) shows the Fock-Darwin energy states as a function of the magnetic field. In strong magnetic fields, a change in the radial quantum number n leads to a much larger energy difference than a change in the angular momentum quantum number m, and thus the energy spectrum separates into Fock-Darwin bands labeled by the quantum number n. If the confinement potential vanishes, the degenerate Landau levels of free 2D electrons in a magnetic field are retrieved. Since apart from the definition of the length scale, the wave functions look exactly the same as for $\omega_0 = 0$, the Fock-Darwin bands are frequently called just Landau levels.

If the magnetic field is strong enough, the higher Landau levels can be neglected as the ground

[3] To avoid possible confusion, note that for $\omega_0 = 0$, the oscillator length reduces to $l = \sqrt{2}\sqrt{\hbar/m^*\omega_c}$, which is the magnetic length widely used in the quantum Hall literature multiplied by $\sqrt{2}$.

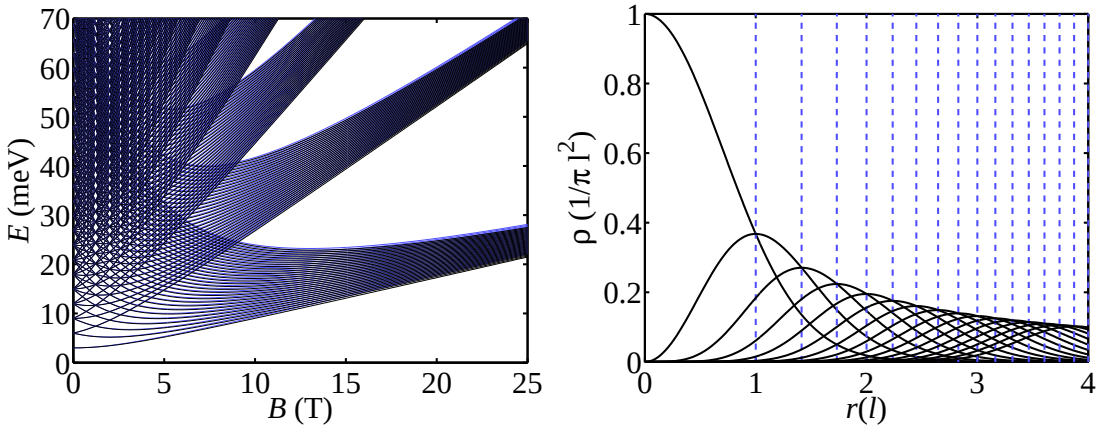

(a) (b)

Figure 2.3: (a) Fock-Darwin energy levels form near-degenerate bands at strong magnetic fields. 30 lowest energies of each of the lowest Fock-Darwin bands of both spin types are shown. The two opposite spins are plotted with different colors but the almost negligible Zeeman splitting is hard to see. The confinement strength is set to 3 meV. (b) Radial probability densities of the first few Fock-Darwin states at strong magnetic field (lowest Landau level) with the maxima at $\sqrt{m}l$.

state has weight mainly for those many-body basis states (Slater determinants) whose all single-particle states lie in the lowest Landau level. This is called the Landau level projection to the lowest Landau level (LLL). Figure 2.3(b) shows first few radial density profiles in the LLL. There is an important relation between the single-particle states and the magnetic flux $\Phi = BA$. The area enclosed by the ring-like LLL single-electron probability densities is $m\pi l^2$. Thus, the magnetic flux through the interior of the dot is given by $\Phi = Bm\pi l^2 \approx mh/e$ (at strong B), so it is approximately quantized in units of the flux quantum $\Phi_0 = h/e$. The wave function of an electron that winds around a magnetic flux tube acquires the Aharonov-Bohm phase factor $e\Phi/\hbar$, which in this case reduces to $2\pi m$ if the electron is in the energy state with angular momentum m. Thus, in some sense, a change in the angular momentum of the system corresponds to tunneling of elementary magnetic flux tubes h/e in and out of the interior of a single-electron quantum dot. In the next section, we examine more closely these magnetically induced vortices and how interactions between the electrons can result in new kind of "particles" that are composites of electrons and vortices. In a somewhat analogous magnetic flux penetrated quantum ring, an electron on the ring gains angular momentum as the flux is increased. However, if the radius of the ring is not proportional to magnetic length l but instead e.g. a constant, the magnetic flux through the ring is not quantized but continuous

though the ground state may change periodically as the flux is increased.

A few remarks about the interactions and spin are in order. First, one way to see that the system is strongly correlated is to look at the energy scales. The correlations due to Coulomb interaction are of the order of magnitude $e^2/4\pi\epsilon l$, which is about 6 meV, 8 meV, and 10 meV at magnetic field equal to 0 T, 5 T, and 10 T, respectively (the parameters are the same as in Fig. 2.3). At the same time, differences in the single-particle excitation energies are only of the order 3 meV, 1 meV, and 0.5 meV. Therefore, the Coulomb interactions are expected to have an effect even without an external magnetic field, while these effects are considerably enhanced by a strong magnetic field.

Second, as seen in Figure 2.3(a), the Zeeman term causes almost negligible spin splitting. However, the total spin is typically not zero even if the Zeeman term is experimentally made to vanish with $g^* \to 0$. Instead, the strong Coulomb interactions between the electrons lead to diverse spin structure and magnetic properties. The Coulomb interactions tend to spontaneously break the approximate spin-symmetry in favor of a spatially antisymmetric wave function that vanishes when electron coordinates coincide. However, depending on the form of the confining potential both ferromagnetism and antiferromagnetism are observed in quantum dots and rings allowing for tunable magnetism.

2.3 Phase vortices and composite particles

In the previous section, it was shown that in a parabolic quantum dot the angular momentum quantization leads to quantization of the magnetic flux piercing the interior of the LLL single-electron states. Since the single-particle angular momentum operator is $\hat{M} = -i\hbar\partial_\theta$, the angular momentum is manifest in the $z^m \propto e^{im\theta}$ factor of the wave function and is therefore related to the number of branch cuts in the phase of the wave function. As noted in Ref. [17], also the vanishing of the probability density at the end of the branch cut is quite a general feature as seen by considering the probability current density for an electron ($\psi = |\psi|e^{i\varphi}$) moving in a magnetic field

$$\mathbf{J}(\mathbf{r}) = \frac{\hbar}{m}\mathrm{Im}\left[\psi^*(\mathbf{r})\nabla\psi(\mathbf{r})\right] + \frac{e}{m}\mathbf{A}(\mathbf{r})\psi^*(\mathbf{r})\psi(\mathbf{r}) = \frac{e}{m}|\psi(\mathbf{r})|^2\left[\frac{\Phi_0\nabla\varphi(\mathbf{r})}{2\pi} - \mathbf{A}(\mathbf{r})\right]. \tag{2.3.1}$$

The term $\nabla\psi(\mathbf{r})$ is singular at the branch point $\mathbf{r}_b$. For the probability current density to be finite there, the probability density $|\psi(\mathbf{r}_b)|^2$ must vanish. This singular circular flow of the probability current density is called a vortex, and a location of a vortex refers to the branch point even though the charge depletion is in reality extended in size.

In a straightforward generalization to a many-electron system, we consider the branch structure of a wave function $\Psi(\mathbf{r}_1, \mathbf{r}_2, \ldots, \mathbf{r}_N)$ with respect to one probe coordinate $\mathbf{r}_i$. To fix the phase conveniently and rescale the often very small Ψ, we define a conditional wave function as

$$\Psi_{\mathrm{c}}(\mathbf{r}) = \frac{\Psi(\mathbf{r}, \mathbf{r}'_2, \ldots, \mathbf{r}'_N)}{\Psi(\mathbf{r}'_1, \mathbf{r}'_2, \ldots, \mathbf{r}'_N)} \,. \tag{2.3.2}$$

By convention, the primed coordinates are optimized such that $|\Psi(\mathbf{r}'_1, \mathbf{r}'_2, \ldots, \mathbf{r}'_N)|$ is maximal although it sometimes is useful to observe the movement of zeros as these coordinates are moved. The definition does not fix the conditional wave function uniquely as there always are several configurations that yield the maximum amplitude. However, if the vortices are considered as holes in the plane, the resulting two-dimensional manifolds are topologically equivalent. If the spin is included, we have $\Psi_{\mathrm{c}}^{\uparrow}$ and $\Psi_{\mathrm{c}}^{\downarrow}$ defined as

$$\Psi_{\mathrm{c}}^{\sigma}(\mathbf{r}) = \frac{\Psi(\mathbf{r}, \sigma, \mathbf{r}'_2, \sigma_2, \ldots, \mathbf{r}'_N, \sigma_N)}{\Psi(\mathbf{r}'_1, \sigma, \mathbf{r}'_2, \sigma_2, \ldots, \mathbf{r}'_N, \sigma_N)} \,. \tag{2.3.3}$$

Here σ_i are fixed as to yield the correct total spin in z-direction.

In analogy with the single-particle case, singularities at the branch points of the conditional wave function are called vortices. In the many-body system, although the conditional density is zero, the electron density is no longer always zero at the vortex core as the positions of the vortices become dependent on the $N-1$ electron coordinates. The details of the many-body wave function determine how sensitive the location of the vortex is to the fixed electrons – whether it is localized, bound to electrons, or something in between. Figure 2.4 illustrates these phase vortices by showing the phase and the logarithmic absolute value contours of the conditional wave function in two spin-polarized systems. In Fig. 2.4(a), there is a three-electron square quantum dot with one vortex on top of each fixed electron and four vortices whirling elsewhere in the system while in Fig. 2.4(b) three vortices lay on top of each fixed electron in a screened parabolic quantum dot.

The vortex structure gives detailed information about the many-body wave function. In the

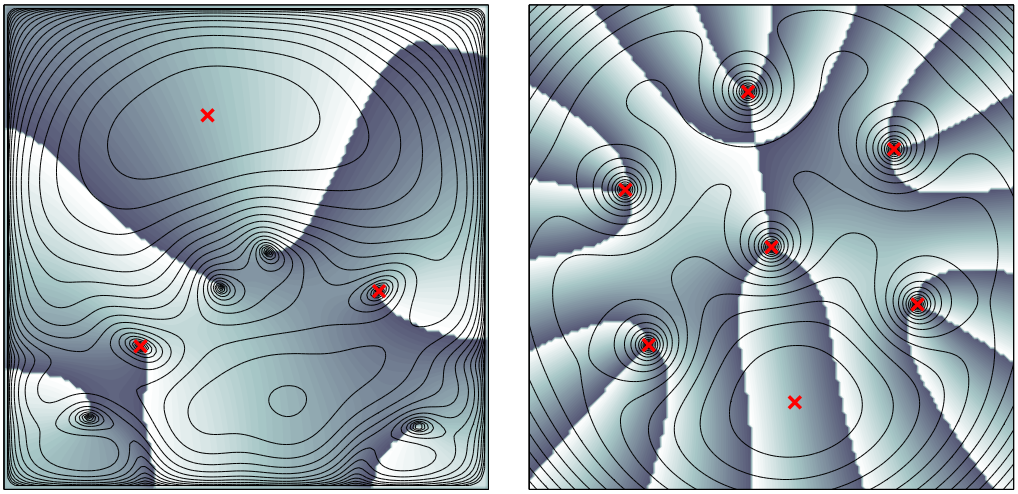

(a) (b)

Figure 2.4: The phase and logarithmic contours of the conditional wave function for (a) three spin-polarized electrons in a square quantum dot interacting through Coulomb interaction and (b) seven spin-polarized electrons in a parabolic quantum dot interacting through screened Coulomb interaction. Positions of the fixed coordinates and the most likely position of the probe electron are marked by red crosses.

fully spin-polarized lowest Fock-Darwin band, the wave function can always be written as

$$\Psi(z_1, z_2, \ldots, z_N) = P_{\Delta M}(z_1, z_2, \ldots, z_N) \prod_{i<j}^{N} (z_i - z_j) \exp\left(-\sum_{i=1}^{N} z_i \bar{z}_i / 2 \right) \qquad (2.3.4)$$

where $P_{\Delta M}$ is a homogeneous symmetric polynomial of order ΔM, meaning that all monomials in the sum are of the same order. The product factor in Eq. (2.3.4) implies that each electron sees a vortex bound to the other electrons (Pauli vortex) while possible additional vortices are in the symmetric polynomial. The total angular momentum of the system is equal to the polynomial order of each term in the factor multiplying the exponential damping, and it is therefore equal to $M = N(N-1)/2 + \Delta M$. The classical minimum energy configuration would be a highly symmetric Wigner molecule where electrons in the simplest case are located at apexes of a regular polygon. This is reflected in the quantum mechanical ground states, which occur at certain magic angular momenta understood as follows [18]. The total angular momentum operator is the generator of rotations of the whole molecule. This in turn can be linked to exchanges of identical fermions, which yields a selection rule for the angular momentum. Thus, for example the ground states occur at $M = N(N-1)/2 + kN$ with $k = 0, 1, \ldots$ for $N < 6$

while for $N \geqslant 6$ more complex classical configurations and hence more angular momenta become available. Even small changes in the confinement potential and the effective interaction can affect the symmetry of the Wigner molecule.

Vortices are a useful and intuitive concept in the study of two-dimensional electron systems, and in particular quantum dots, in a magnetic field [19,20]. When the magnetic field is tuned or the system is perturbed in a manner equivalent to a small change in the confinement potential, the underlying complicated many-body physics and collective excitations are often understood just by looking at changes in the vortex structure of conditional wave functions.

As noted in the previous section, the Coulomb interaction energy of electrons in the quantum dot increases with the magnetic field. At a ground-state transition point, it becomes favorable to compensate the squeeze of the magnetic field by an increase in the total angular momentum and thus the number of vortices. Since a vortex is associated with a charge depletion, it tends to locate at those places that electrons avoid either due to inter-electron correlations or because of the single-particle potential landscape.

Typically a vortex is created near the center-of-mass of the parabolic quantum dot giving rise to a collective excitation where the total interaction energy decreases as the angular momentum of each electron increases by one. If enough vortices are available, a short-range repulsive interaction between the electrons causes the vortices to bind near the electron positions thus decreasing the interaction energy [21]. This is why the vortices can be bound exactly to the electron coordinates in Fig. 2.4(b). The relatively accurate Laughlin's trial wave function for a set of strongly correlated fractional quantum Hall states at filling fractions $\nu = 1/(2m+1)$ with $m = 0, 1, 2, \ldots$ has the form

$$\Psi(z_1, z_2, \ldots, z_N) = \prod_{i<j}^{N} (z_i - z_j)^{2m+1} \exp\left(-\sum_{i=1}^{N} z_i \bar{z}_i / 2 \right) , \tag{2.3.5}$$

in which, besides the Pauli vortex, $2m$ additional vortices bind to electrons forming composite-particles. Alternatively, one can say that a single vortex of winding number $2m+1$ is bound to each electron. In the case of a long-range pure Coulomb interaction, there are other competing correlations and thus the vortices, while bound to electrons, are separated by a small distance. For a finite-thickness effective interaction weakened at short distances, the long-range correlations dominate and binding of vortices becomes even weaker leading to destruction of fractional

quantum Hall effect (see next section) in thick systems [22].

As seen in Fig. 2.4(a),vortices are a robust concept applicable even when the rotational symmetry is broken by confining the electrons to a rectangle. In Fig. 2.4(a), we have two vortices of the center-of-mass type, which are still weakly bound to electrons. Related to this binding are the two additional vortices at the lower corners of the rectangle, a position that is disfavored by electrons orbiting around the rectangle.

Above, all the vortices rotate in the same direction as they are due to holomorphic factors z in the wave functions. In the higher Landau level, the wave function can also have anti-holomorphic factors $\bar{z}$ giving rise to anti-vortices. However, only vortices are relevant to the present work as anti-vortices are typically not seen even in the presence of a significant Landau level mixing. Instead, one can have a quasielectron that manifests itself as a factor $\prod_i \partial/\partial z_i$ in the polynomial part of the many-body wave function and thus as a lack of a vortex.

2.4 Quantum Hall phases and topological order

It was the year 1980 when von Klitzing found the quantum Hall effect while performing characterization of the electronic transport of silicon field-effect transistors at the High Magnetic Field Laboratory in Grenoble [23]. What exactly he did find using a device sketched in the inset of Figure 2.5(a) are plateaus of constant transverse resistance R_{xy} and simultaneously vanishing diagonal resistance R_{xx} as a function of the gate voltage that sets the electron concentration n in the 2DEG (similar plateaus are observed as a function of magnetic field for constant n). Due to the Lorentz force, the relation between the current and voltage is of the tensor form

$$\begin{pmatrix} V_x \\ V_y \end{pmatrix} = \begin{pmatrix} R_{xx} & R_{xy} \\ R_{yx} & R_{yy} \end{pmatrix} \begin{pmatrix} I_x \\ I_y \end{pmatrix} . \tag{2.4.1}$$

Remarkably, the quantization of R_{xy} is universal and thus independent of any sample dependent parameters while it occurs at $R_{xy} = h/\nu e^2$ with integer ν where h is the Planck's constant and e is the elementary charge [24, 25]. In fact, R_{xy} attains these values so accurately that it is now used as a resistance standard and in resistance calibrations. The constancy of the resistance tensor at finite gate voltage intervals implies that the induced electrons do not contribute to the current but are localized to impurities and inhomogeneities of the sample. The integers ν

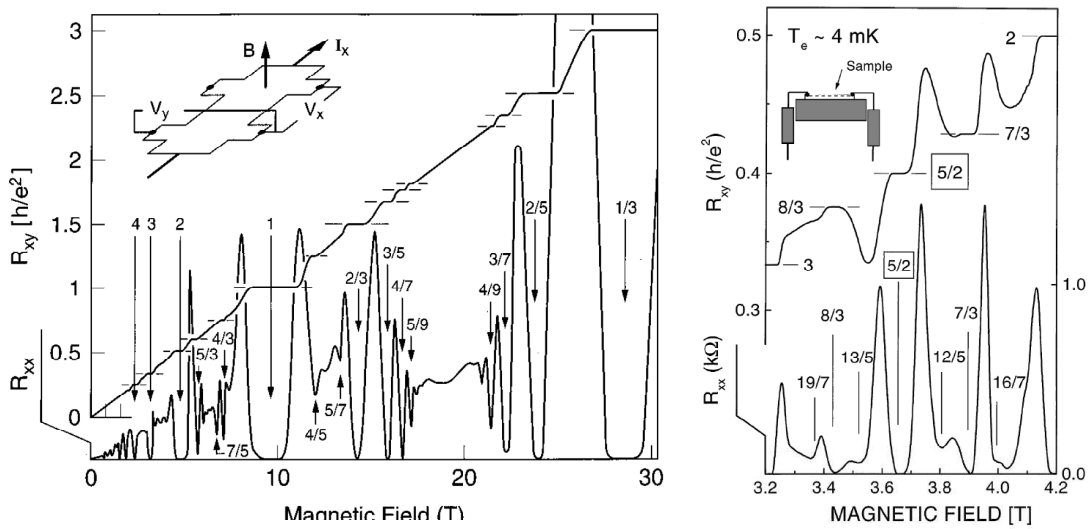

(a) (b)

Figure 2.5: (a) Composite view of the transverse resistance R_{xy} and the diagonal resistance R_{xx} of 2D electron gas of density $n = 2.33 \times 10^{11}$ cm^{-2} as a function of the magnetic field at a temperature T of 85 mK. Instead of a linear behavior, R_{xy} exhibits plateaus whose inverse corresponds to fractions $\nu = p/q$ indicated in the figure. The integer ν are hallmark of the Landau quantization of the single-electron states in the magnetic field while the existence of fractional ν is of many-particle origin. Adapted from Stormer *et al.* [5]. (b) Another sample at $T = 4$ mK showing the weak plateau with $\nu = 5/2$. Adapted from Pan *et al.* [27].

called filling factors then follow from the Landau quantization as each occupied Landau level contributes to the conductance an additive term e^2/h. The integer quantum Hall effect (IQHE) is thus understood essentially in terms of Landau quantization of non-interacting electrons in the presence of disorder although some more recent theoretical work points out the importance of electron-electron interaction in the plateau transitions (see e.g. Ref. [26] and references therein).

Therefore, it was all the more unexpected when two years later Tsui, Störmer, and Gossard reported an observation of a plateau at $\nu = 1/3$, a fractional filling factor for which the above description does not apply [28]. To date, many more fractional quantum Hall filling factors (or filling fractions) have been observed as cleaner experimental samples are available [5, 29]. Figure 2.5(a) and (b) show experimental resistances as a function of the magnetic field where some of the observed filling factors are indicated.

In the IQHE picture, the fractional ν corresponds to the situation with a partially filled non-interacting Landau level. Due to the massive degeneracy of the single-particle states, the ef-

fect of interactions is enhanced to the extreme, and indeed the fractional quantum Hall effect (FQHE) is caused by the Coulomb interactions between the electrons. At certain special filling fractions, the interactions induce a mobility gap analogous to the mobility gap between the Landau levels, which again with little disorder makes possible the finite extent of the plateaus.

How exactly do the interactions cause the gap is a question that the theory strives to answer. The first explanation was given by Laughlin [30, 31] who utilizing an analogy with a classical plasma devised model wave functions supported by an exact diagonalization study with a computer that explained the fractions $\nu = 1/(2m+1)$ [cf. Eq. (2.3.5)]. Subsequently, Haldane [32], Halperin [33], and Jain [34] came up with theories to explain the other odd-denominator filling fractions. Most consistent with experiments is the Jain's picture of composite-fermions that exhibit IQHE [35].

However, there are still observed fractions, most evident of which is the even-denominator one at $\nu = 5/2$ [Fig. 2.5(b)], that stipulate a different explanation, and so far no consensus has been reached on what this correct description would be. In the light of numerical calculations and recent experiments [36,37], a particular model based on p-wave pairing of composite-fermions [38, 39] (and its particle-hole conjugate [40–42]) has been a strong candidate for the $\nu = 5/2$ plateau. In this model, the lowest Landau level of both spin-types is assumed occupied ($\nu = 2$) and inert while the second Landau level is half-filled and spin-polarized ($\nu = 1/2$). What makes this plateau particularly interesting is the possibility that its quasiparticle excitations (see the next section) might be useful for quantum information devices. We have assessed the stability of this so called Pfaffian model in confined geometries – something that would be important for experimental probing of the state. In the experimental set-ups, such as quantum point-contacts, the electrons are constrained to a narrow strip and subject to Landau level mixing (rather than an infinite plane with the electron states projected to the spin-polarized second Landau level), which along with the form of the effective interaction can affect the stability. The results show that while an optimized form of the confinement potential and effective interaction ideally favor the Pfaffian state, there is a competing spin-droplet formation that may fill the second Landau level compactly, disallowing entirely the higher angular momentum required by the Pfaffian state.

There is something peculiar about the fractional quantum Hall states that distinguishes them from other seemingly exotic phases of matter such as the superconducting state. Although dif-

ferent fractions correspond to different phases of matter, the phase transition from one phase to another is not related to a symmetry breaking as in conventional phase transitions [43]. Moreover, the order parameter of an FQH state is off-diagonal and obtained after a non-local singular gauge transformation showing that the FQH states exhibit complicated long-range quantum entanglement related to topological properties of the state [44]. This leads to the main reason behind the recent grown interest in the fractional quantum Hall states. It has been proposed that the topological robustness of this type of matter and in particular the topological properties of the quasiparticle excitations could be utilized in preparing devices that are resistant to the decoherence caused by local interactions with the environment. Such considerations are important as decoherence is a primary obstacle in pursuits to build a quantum computer that is a computer which by utilizing the quantum entanglement would perform certain tasks exponentially faster than classical computers [45, 46].

2.5 Quasiparticles and fractionalization

Being one of the few known ways to simplify the many-body problem, quasiparticles are an important concept in condensed-matter physics. They may be closely related to elementary particles such as the quasielectrons in solids, for which the interaction of the electron with the crystal lattice is taken into account by the dispersion relation and effective mass of the quasielectron. Alternatively, they can be emergent collective phenomena such as phonons, the quanta of sound waves related to the vibration of atoms in a crystal.

Returning to our two-dimensional system of strongly correlated electrons in a magnetic field, several types of quasiparticles can be identified. First, the effective Hamiltonian Eq. (2.2.1) describes no real electrons but such electrons, for which the band structure of the semiconductor and the planar confinement are taken into account by the effective mass and effective interaction. As described previously, the interactions between these electrons give rise to two different types of quasiparticles: isolated vortices and composite-particles. In addition, there are quasiparticles at the edge of the system such as gapless phonon modes and in non-Abelian quantum Hall states also neutral fermionic modes termed Majorana fermions [47, 48]. For the purposes of this work, most important are the quasiparticles associated with localized vortices, and we will briefly discuss them in the following.

Because vortices are associated with a charge depletion and hence a positive charge, they are termed quasiholes conveying a lack of electron density compared to a more fundamental ground state with no vortices. Interestingly, in the fractional quantum Hall regime, the charge associated with a quasihole excitation is typically non-integer and smaller than the elementary charge. Moreover, the precise value of the quasihole charge converges to some specific fractional number as the number of electrons becomes large, the value of which depends on the topological properties of the fractional quantum Hall phase [31]. Since the observation of the fractional charge in 1997 by Picciotto *et al.* [49] and Saminadayar *et al.* [50], measuring the quasiparticle charges from the shot-noise in a quantum-point-contact quasiparticle-tunneling experiment has become a standard technique. This is of great benefit as the quasiparticle charge predictions of theories can now be directly tested, and thus for example the quasiparticle charge at $\nu = 5/2$ is found to be $e/4$ [51, 52].

The fractional charge is a working concept even in small quantum Hall droplets interacting with realistic interactions. Even if the charge of the quasihole (vortex), localized to an area with diameter of the order of magnetic length, has not converged to its thermodynamic-limit value, it remains constant for a fixed electron number in a given phase even when the quasihole is moved and breaks the rotational symmetry [53].

In quantum Hall systems, fractional statistics is a direct consequence of fractional charge [54]. This means that instead of a fermionic or bosonic phase factor ± 1, an interchange of two quasiparticles yields a complex phase factor $e^{i\theta}$ with any statistical angle θ, hence the name anyons [55, 56]. Furthermore, if the ground state of the system with a set of quasiparticles is degenerate, different braidings of quasiparticles can lead to non-commutative unitary transformations in the degenerate subspace [38]. In this case, the statistics is said to be non-Abelian. These so called non-Abelian quantum Hall states have been a topic of great interest during the past ten years due to the intriguing possibility that their unitary transformations and topological stability could be utilized in fault-tolerant quantum information processing [57, 58].

Substantial progress has occurred lately on the experimental front as the Abelian fractional statistics of the Laughlin quasiparticles has been well confirmed [59]. Moreover, the analysis due Bishara *et al.* [60] of recent experiments by Willett *et al.* [52] suggests that the interferometric signatures observed in the experiment are most likely due to non-Abelian statistics of the quasiparticles.

2.6 Physics at the edge

In the quantum Hall effect, the interior of the sample (bulk) has a mobility gap at the Fermi energy so that only the states at the edge of the sample can contribute to the current transport. As the low-energy degrees of freedom lie at the edge, understanding of the detailed properties of the edge states is of fundamental importance for the experimental studies that aim to probe the quasiparticle properties, or otherwise identify the correct description, of for example the $\nu = 5/2$ state.

The edge states were studied early on in the context of IQHE [61]. However, there is a significant difference between the IQHE and FQHE edge states. In the former case, the mobility gap in the bulk is of single-particle origin and thus the quasiparticles at the edge reflect Fermi-liquid character [61]. In the latter case, the mobility gap is due to many-particle interactions and this also affects the edge modes, which are entangled with the rest of the state in the bulk. Wen has argued that the edge of an Abelian FQHE state is described by a chiral Tomonaga-Luttinger liquid [62]. More generally, the edge states can be described by $1+1$-dimensional conformal field theories [58].

In any case, from the edge theories it is possible to calculate the probability for an electron to propagate a distance x along the edge in time t, which is given by the Green's function. Its asymptotic behavior is found to be

$$\langle \psi^\dagger(x,t)\psi(0,0)\rangle \propto (x - vt)^{-g} \,, \tag{2.6.1}$$

where v is the velocity and the value of the exponent g depends on the filling fraction ν [62]. The exponent g is further related to the zero temperature current-voltage characteristics of a metal-insulator-FQH junction as

$$I \propto V^g \,. \tag{2.6.2}$$

The experiments indeed find a non-Ohmic current-voltage dependence in accordance with the Luttinger liquid theory. However, the measured tunneling exponent appears to be smaller than the predicted value and varies linearly with the magnetic field at a plateau corresponding to a given filling fraction [63].

Among the many considered explanations [64], analysis of Wan *et al.* [65] based on micro-

scopic simulations suggests that the smaller value of the tunneling exponent is due to the edge confinement. One can also see that the tunneling exponent additionally varies in the $\nu = 1/3$ plateau in qualitative agreement with the experiments as the magnetic field changes (see e.g. Publication **V**) while the position of the edge confinement potential and electron number is held constant. This may be one factor in the non-universality of the exponent.

Chapter 3

Computational methods

The major computational problem in this work is finding the ground states of the effective mass Hamiltonian of Eq. (2.2.1) in different type of nanostructures and at different system parameters. Because of the interaction term in the Hamiltonian, exact analytic solutions can not generally be obtained. Moreover, the correlations between the confined electrons are so strong that the Hartree-Fock method and perturbation theory fail to give the correct physics. This can be explicitly seen for example in Figs. 1 and 2 of Publication **VIII** where both of these methods (HF and BW) clearly deviate from the exact solution (CI). Thus, the proper analysis of these nanostructures requires that the electron correlations are treated non-perturbatively. Although there exist some special situations, typically in two-particle or one-dimensional many-particle systems or with unrealistic interaction potential, where interactions can be treated analytically, in practice, we have to resort to a numerical calculation.

There are several numerical schemes that are routinely employed in the condensed matter electronic structure calculations and quantum chemistry. These include the famous density-functional methods [66] and the Hartree-Fock method with its descendants [67]. However, those methods that are able to treat large systems in feasible time are typically achieving it by neglecting and approximating electron correlations. While this is completely legitimate in many systems where the correlations are indeed weak, in our system of interest the correlations can be extremely strong and thus many of the commonly used techniques have a limited applicability.

In this chapter, we will briefly review the computational techniques that are employed in the

Publications **I-VIII**.

The exact diagonalization method (Sec. 3.1), which also goes by the name configuration interaction, is the most accurate method being practically exact for small systems. Even though the maximum number of electrons that can be treated with this method is of the order of ten, it can still be regarded as the so far most successful numerical method in the study of quantum Hall systems. In addition to the high accuracy, this owes particularly to the fact that the method yields the whole many-body wave function, whose topological structure (such as vortices, composite-particles, and fractional charges) and overlap with candidate trial wave functions can be readily examined.

The density-functional theory (Sec. 3.2), on the other hand, is a very powerful method in handling large system sizes. The main idea is to describe the system in its ground state not by the many-body wave function but merely by the electron density. The method is now widely used in both solid-state physics and chemistry to determine properties of solids and large molecules. However, due to the approximation done at choosing the density-functional, caution is called for when applying the method to a system with complicated correlations. In particular, the method does not work very well at the extremely strongly correlated low filling fraction phases of fractional quantum Hall systems.

The reduced density-matrix functional theory (Sec. 3.3) extends the density-functional theory such that the fundamental object is now the slightly more complicated reduced density-matrix. Although the method entails some obvious advantages compared to the traditional density-functional theory, it has only recently developed to a point where it can be expected to be useful for realistic applications.

Finally, the quantum Monte Carlo methods (Sec. 3.4) are a class of algorithms relying on the Monte Carlo integration technique that allows efficient calculation of high-dimensional integrals. A scheme known as the variational quantum Monte Carlo is applied in Publication **III** while observables are extracted from the many-body wave function by the Monte Carlo integration in Publication **VIII**.

3.1 Exact diagonalization

Exact diagonalization is a robust and straightforward numerical method to obtain eigenvalues and eigenstates of quantum mechanical observables.

The state vector $|\Psi\rangle$ that describes a quantum mechanical system belongs to a Hilbert space $\mathcal{H}$, which is typically infinite dimensional. The states we are interested in solve the time-independent Schrödinger equation $H|\Psi\rangle = E|\Psi\rangle$ and are therefore the eigenvectors of the Hamiltonian operator $H : \mathcal{H} \to \mathcal{H}$. To obtain them, we construct the matrix $H_{ij} = \langle\Phi_i|H|\Phi_j\rangle$ that tells how the operator acts in a given basis $\{|\Phi_i\rangle\}_{i=0}^{\infty} \subset \mathcal{H}$ and simply truncate (if it is infinite or otherwise too large) and diagonalize it.

The most decisive phase in solving a given problem with exact diagonalization is the choice of the basis as there are really no options at the later stages. An ideal basis is physically motivated and mathematically convenient so that the eigenvectors obtained with a truncated basis are close to what the exact eigenvectors would be while the matrix elements H_{ij} can be calculated analytically or at least otherwise efficiently. The lowest eigenstates of the non-interacting problem form a physically motivated natural basis. However, the matrix elements of the interaction operators in H then typically need a numerical treatment. Fortunately, the four dimensional Coulomb integrals can often be reduced into lower dimensional integrals by Fourier or Hankel transforms [68]. The Fock-Darwin states [Eq. (2.2.3)] are a convenient exception, for which all the matrix elements can be obtained in a closed form [17, 69]. Furthermore, in the exact diagonalization approach, the Landau level projection applicable in the strong magnetic field regime means that we truncate the basis to one Fock-Darwin band. In that case the Landau level index of each electron is conserved. Typically, also the total angular momentum or spin is conserved, and solving the problem in each thus constrained subspace of $\mathcal{H}$ greatly accelerates the computation.

A practical implementation for the construction of the Hamiltonian relies on the second quantized formalism of quantum mechanics. A fermionic occupation number state related to single-particle basis $\{\psi_i\}_{i=0}^{k}$ is denoted $|n_0, n_1, \ldots, n_k\rangle$ with $n_i \in \{0, 1\}$ and $\sum_i n_i$ equal to particle number N. It corresponds to the result of antisymmetrizing the product wave function $\psi_{i_0}(1)\psi_{i_1}(2)\ldots\psi_{i_N}(N)$ where the numbers denote the coordinates (e.g. spin and spatial) and indices $i_0 < i_1 < \ldots < i_N$ correspond to the N occupied single-particle orbitals $n_{i_j} = 1$. The

anticommuting operators $a_i^\dagger$ and a_i create and annihilate occupations and the second quantized Hamiltonian can be written using them as

$$H = \sum_{i,j} \langle i|H_1|j\rangle a_i^\dagger a_j + \frac{1}{2} \sum_{i,j,k,l} \langle i,j|H_2|k,l\rangle a_i^\dagger a_j^\dagger a_l a_k \; . \tag{3.1.1}$$

Here $\langle i|H_1|j\rangle$ are the matrix elements due to kinetic energy and external potentials while $\langle i,j|H_2|k,l\rangle$ are the interaction matrix elements, and the first quantized Hamiltonian is separated accordingly into one and two-particle operators

$$H = \sum_{\alpha=1}^{N} H_1(\alpha) + \frac{1}{2} \sum_{\alpha,\beta\neq\alpha}^{N} H_2(\alpha,\beta) \; . \tag{3.1.2}$$

The occupation number states can be stored into the computer memory as integers using the bit presentation such that for example $|101010\rangle$ corresponds to bit sequence $101010_2 = 2 + 8 + 32 = 42$. The operations needed in the calculation of the matrix elements of the Hamiltonian such as $\langle n_0, n_1, \ldots, n_k|a_i^\dagger a_j^\dagger a_l a_k|n_0', n_1', \ldots, n_k'\rangle$ can then be efficiently performed using bit operations. This is important since the construction of the Hamiltonian is usually the most time consuming part of the calculation.

Eventually, we can extract the eigenvalues and eigenvectors of the sparse matrix H_{ij}. As the many-body basis size grows exponentially with the electron number, the matrix H_{ij} becomes very large if we want to have about as many electrons as we can handle. Fortunately, one is frequently interested only in the ground state or a few lowest-lying excited states that can be obtained efficiently with the Lanczos algorithm [70]. In this algorithm, starting with a random vector $|R\rangle$, an orthogonal basis for the K-dimensional Krylov subspace spanned by vectors $\{H^i|R\rangle\}_{i=0}^{K-1}$ is formed (typically $K \ll \dim|R\rangle$) and utilized to yield a near exact approximation for the lowest eigenvalues and eigenvectors of H_{ij}.

Our implementation of the exact diagonalization is written in Fortran programming language and utilizes the Linear Algebra Package [71].

Since the early days [31, 32, 72, 73], the exact diagonalization has been a central tool in the understanding of fractional quantum Hall effect. Even if the electron number is rather restricted, studies in different types of manifolds (mainly torus, sphere, or disc) have allowed accurate modeling of the physics in a single Landau level. For example, akin to our work in

disc, Refs. [74, 75] have studied on sphere the dependency of the stability of the non-Abelian quantum Hall states on the form of the electron interaction. However, current research directions call for larger electron numbers due to the need for inclusion of multiple Landau levels and Landau level mixing [76]. One alternative is to try to extend the exact diagonalization to larger systems with the density matrix renormalization group method [77]. Another alternative is to employ the techniques represented in the following sections.

3.2 Density-functional theory

The density-functional theory is based on the Hohenberg-Kohn theorem (1964) [78], which states that for an interacting many-electron system described by the Hamiltonian

$$H = \sum_{i=1}^{N} \left[-\frac{\hbar^2}{2m}\nabla^2 + V_{\rm ext}(\mathrm{r}_i) \right] + \sum_{i<j}^{N} \frac{e^2}{4\pi\epsilon|\mathbf{r}-\mathbf{r}'|} \,, \tag{3.2.1}$$

there is a one-to-one correspondence between the external potential $V_{\rm ext}(\mathbf{r})$ and the density $n(\mathbf{r})$ of a non-degenerate ground state, and in addition that there exists a universal functional $F[n]$ such that the minimization of the energy functional

$$E[n] = \int d\mathbf{r} n(\mathbf{r}) V_{\rm ext}(\mathbf{r}) + F[n] \tag{3.2.2}$$

with respect to n yields the exact ground-state energy and density. The minimization is among all ground-state densities that can come out of Eq. (3.2.1) for some external potential and particle number N.

In the Kohn-Sham formulation [79], the energy functional [Eq. (3.2.2)] is written as

$$E[n] = T_{\rm s}[n] + V_{\rm s}[n] \,, \tag{3.2.3}$$

$$V_{\rm s}[n] = \int n(\mathbf{r}) V_{\rm ext}(\mathbf{r}) d\mathbf{r} + \frac{1}{2}\int \frac{n(\mathbf{r})n(\mathbf{r}')d\mathbf{r}d\mathbf{r}'}{|\mathbf{r}-\mathbf{r}'|} + E_{\rm xc}[n] \,, \tag{3.2.4}$$

where $T_{\rm s}[n]$ is the kinetic energy of N non-interacting electrons moving in an effective potential

$$V_{\rm s}(\mathbf{r}) = \frac{\delta V_{\rm s}[n]}{\delta n(\mathbf{r})} = V_{\rm ext}(\mathbf{r}) + \int \frac{n(\mathbf{r}')d\mathbf{r}'}{|\mathbf{r}-\mathbf{r}'|} + \frac{\delta E_{\rm xc}[n]}{\delta n(\mathbf{r})} \,. \tag{3.2.5}$$

Thus the ground-state density $n(\mathbf{r}) = \sum_{i=1}^{N} |\psi_i(\mathbf{r})|^2$ can be obtained by solving self-consistently the N lowest eigenstates $\{\psi_i\}_{i=1}^{N}$ of a non-linear single-particle Schrödinger equation

$$\left[-\frac{\hbar^2}{2m}\nabla^2 + V_{\mathrm{s}}(\mathbf{r})\right]\psi_i(\mathbf{r}) = \epsilon_i\psi_i(\mathbf{r}) \;, \tag{3.2.6}$$

where the non-linearity arises from the dependence of the potential $V_{\mathrm{s}}(\mathbf{r})$ on the density. The energies ϵ_i of the Kohn-Sham orbitals ψ_i are not directly physical but related to the total energy E by

$$E = \sum_{i=1}^{N}\epsilon_i - \frac{1}{2}\int\frac{n(\mathbf{r})n(\mathbf{r}')d\mathbf{r}d\mathbf{r}'}{|\mathbf{r}-\mathbf{r}'|} + E_{\mathrm{xc}}[n] - \int n(\mathbf{r})\frac{\delta E_{\mathrm{xc}}[n]}{\delta n(\mathbf{r})}d\mathbf{r} \;. \tag{3.2.7}$$

Nevertheless, both the Kohn-Sham orbitals and energies give at least qualitative information that is valuable in many applications [80].

The above described early rudimentary density-functional theory has later been generalized to handle non-zero magnetic fields, current, spin, as well as degenerate ground states, time-dependence, and excitations. In any case, the exact form of $E_{\mathrm{xc}}[n]$ is only known for certain limiting cases, and it must in practice be approximated. In physics, the most widely used approximation is the local density approximation, in which the exchange correlation energy density at a point $\mathbf{r}$ depends only on the electron density at that same point $n(\mathbf{r})$. In the local spin density approximation, the different spin components are taken into account so that

$$E_{\mathrm{xc}}[n_\uparrow, n_\downarrow] = \int n(\mathbf{r})\epsilon_{\mathrm{xc}}(n_\uparrow(\mathbf{r}), n_\downarrow(\mathbf{r}))d\mathbf{r} \;. \tag{3.2.8}$$

In applications, the exchange correlation energy density is almost exclusively taken to be that of a uniform homogeneous electron gas. It is then further separated into exchange and correlation energy densities $\epsilon_{\mathrm{xc}} = \epsilon_{\mathrm{x}} + \epsilon_{\mathrm{c}}$, first of which is known analytically. We employ in Publication **III** the quasi-two-dimensional local spin density approximation with the parametrization of the correlation energy density ϵ_{c} obtained with diffusion quantum Monte Carlo by Attaccalite *et al.* [81].

The density-functional theory has been applied extensively in study of quantum dots [82–84], and is found to work well at weak magnetic fields where the electron correlation is not too strong. In particular, the Landau level mixing causes no additional difficulties. However, present

functionals perform weakly at the strongly correlated regime, which is reflected in the incapability to produce flat enough electron densities e.g. at fractional quantum Hall filling fraction $\nu = 1/3$. This is the motivation behind the method presented in the following section.

3.3 Reduced density-matrix functional theory

Because fermion and boson wave functions are antisymmetric with respect to change of coordinates, the expectation values of physical operators, which are sums of terms depending on one or two coordinates, can be expressed in a more compact form using the reduced density-matrices

$$\gamma(\mathbf{r},\mathbf{r}') = N\int \Psi^*(\mathbf{r},\mathbf{r}_2,\ldots,\mathbf{r}_N)\Psi(\mathbf{r}',\mathbf{r}_2,\ldots,\mathbf{r}_N,)d\mathbf{r}_2\ldots d\mathbf{r}_N\ , \tag{3.3.1}$$

$$\Gamma(\mathbf{r}_1,\mathbf{r}_2;\mathbf{r}_1',\mathbf{r}_2') = N(N-1)\int \Psi^*(\mathbf{r}_1,\mathbf{r}_2,\ldots,\mathbf{r}_N)\Psi(\mathbf{r}_1',\mathbf{r}_2',\mathbf{r}_3,\ldots,\mathbf{r}_N,)d\mathbf{r}_3\ldots d\mathbf{r}_N\ . \tag{3.3.2}$$

The one-body reduced density matrix (1-RDM) γ can be obtained from the two-body reduced density-matrix (2-RDM) Γ so that the ground-state energy of e.g. the basic Hamiltonian [Eq. (3.2.1)] can be written as a functional of the 2-RDM

$$E[\Gamma] = \int \delta(\mathbf{r}-\mathbf{r}')\left[\frac{-\hbar^2}{2m}\nabla^2 + V_{\text{ext}}(\mathbf{r})\right]\gamma(\mathbf{r},\mathbf{r}')d\mathbf{r}d\mathbf{r}' + \int \frac{\Gamma(\mathbf{r},\mathbf{r}';\mathbf{r},\mathbf{r}')d\mathbf{r}d\mathbf{r}'}{8\pi\epsilon|\mathbf{r}-\mathbf{r}'|}\ . \tag{3.3.3}$$

If we could easily minimize the energy with respect to the 2-RDM Γ, the ground state of the N-body problem would, for all practical purposes, be solved. However, the reduced density-matrices have a long history dating even back to Dirac [85, 86], and it is found that the conditions (N-representability) for the exact allowed set of the 2-RDM Γ are so complicated that the approach is not feasible. One approach is to extend the set of allowed 2-RDMs by allowing some unphysicality (violation of k-representability for $k \leq N$). This technique has recently been applied to quantum dots by Rothman *et al.* [87], however, it is computationally too heavy for large systems.

On the other hand, the necessary and sufficient N-representability conditions of 1-RDM are very simple: for identical fermions the eigenvalues of the reduced density-matrix must be in the interval $[0, 1]$ and their sum equal to the particle number N. Gilbert's theorem (1975) generalizes the Hohenberg-Kohn theorem to nonlocal external potentials [88]. In the more general

case, a nondegenerate ground state energy is obtained by minimizing a universal functional of the 1-RDM. Again, this functional is not known but approximated. Nonetheless, contrary to the prior, the functional for the kinetic energy is now exact [see first term in Eq. (3.3.3)]. Moreover, once we have obtained the 1-RDM, we can calculate the expectation value of any one-body operator in the ground state. As the 1-RDM is a nonlocal quantity, it should be easier to write down a more accurate approximate energy functional out of it than of the bare electron density.

An approximate interaction energy functional is typically written as

$$V_{\mathrm{ee}}[\gamma] = \frac{e^2}{8\pi\epsilon}\left[\int \frac{\gamma(\mathbf{r},\mathbf{r})\gamma(\mathbf{r}',\mathbf{r}')d\mathbf{r}d\mathbf{r}'}{|\mathbf{r}-\mathbf{r}'|} - \sum_{i,j} f(n_i,n_j)\int \frac{\phi_i^*(\mathbf{r})\phi_j^*(\mathbf{r}')\phi_j(\mathbf{r})\phi_i(\mathbf{r}')d\mathbf{r}d\mathbf{r}'}{|\mathbf{r}-\mathbf{r}'|}\right], \tag{3.3.4}$$

where n_i are the eigenvalues of γ (natural occupation numbers) with corresponding eigenvectors ϕ_i (natural orbitals). For this reason, the method is also called natural orbital functional theory. By different choices of the function $f(n_i, n_j)$, one obtains different approximate functionals.

Although the ideas are not new, only in the last two decades has the reduced density-matrix functional theory been exploited in practical applications. Apart from us, the method has been applied to small atoms and molecules, and more recently to the homogeneous electron gas [89, 90]. The energy functionals have developed, and the current best functionals can be used for quantum chemical applications [91, 92]. Our results indicate that the natural orbital functionals can describe quantum dots, at least in the strongly correlated regime, better than density functionals so that this appears a promising method to test for other nanostructures as well.

3.4 Quantum Monte Carlo

Quantum Monte Carlo (QMC) methods consist of several different techniques based on random sampling and the central limit theorem. Due to accurate treatment of electron correlations and the capability to handle large systems, they offer data that could not be obtained in any other way. Common to these methods is that high-dimensional integrals arise, and they are computed

with the Monte Carlo integration. In the study of electrons in solids [93], variational Monte Carlo (VMC) and diffusion Monte Carlo (DMC) are the most commonly used approaches and are both applicable to quantum dots in a magnetic field [94].

In the variational Monte Carlo, we first generate a trial many-body wave function that depends on a set of parameters α. The energy of the wave function is obtained by the high-dimensional integral

$$E_\alpha = \frac{\int \Psi_\alpha^* H \Psi_\alpha d\mathbf{r}_1 d\mathbf{r}_2 \dots d\mathbf{r}_N}{\int \Psi_\alpha^* \Psi_\alpha d\mathbf{r}_1 d\mathbf{r}_2 \dots d\mathbf{r}_N} , \tag{3.4.1}$$

which according to the variational principle is an upper bound for the exact ground state energy. Minimization with respect to α can be done with the aid of Monte Carlo integration and yields an upper bound for the ground-state energy and an approximate ground-state wave function. The wave function obtained by VMC can be further refined by applying fixed-node DMC or fixed-phase DMC if the time-reversal symmetry is broken [95]. However, the strength of the VMC method derives from the fact that relatively simple trial wave functions typically lead to a high accuracy. However, in the fractional quantum Hall regime the construction of trial wave functions becomes tedious as due to the domination of interactions they are fundamentally of many-body nature. Thus, it becomes difficult to determine ground states accurately from the first principles, yet the Monte Carlo integration can be useful to extract data from analytic trial wave functions that are otherwise well-established (for example by exact diagonalization studies with small systems).

In Publication **III**, the accuracy of the DFT calculations concerning spin-droplet formation is established by comparison to VMC results, and a good agreement is found at the regime of calculations. For details of the VMC method, see Ref. [94]. We do not have a good parametrized trial wave function that would yield accurate results in the FQHE regime. Therefore, in Publication **VIII**, we obtain the occupation numbers of natural orbitals from the parameter-free Laughlin's trial wave function by the Monte Carlo integration. These are then compared to the results of the reduced density-matrix functional theory for large systems, which are found to agree well with the VMC results.

Despite the limitations, Monte Carlo methods are very competitive and compelling. A few of their applications include the study of narrow quantum Hall channels [96], composite fermions and Landau level mixing [97] as well as study of non-Abelian statistics [98] and spin order [99] in paired quantum Hall states.

Chapter 4

Summary

Quantum dots and extended quantum rings formed at semiconductor heterostructures offer both a computational and an experimental laboratory to study two-dimensional electron systems in a magnetic field. In addition to the potential future technological applications of these nanoscale systems in quantum information processing, their study bears significance to the theory of quantized Hall effects.

In the Publications **I**-**VIII**, we have investigated the magnetic and electronic properties of two-dimensional quantum dots and extended quantum rings. The contents are summarized in the following.

Publication **I** inspects the magnetic properties of a non-circular two-electron square quantum dot. We find periodic spin oscillations as a function of the magnetic field and approximate angular momentum quantization generated by splitting of Pauli-vortices. As the vortices carry quantized angular momentum, the abrupt birth of vortices naturally explains the plateaus and jumps of the angular momentum.

In Publication **II**, magnetism and persistent currents are investigated in a lattice model of extended quantum ring. The results suggest the possibility of antiferromagnetic to ferromagnetic switching from strictly 1D to extended quantum ring systems. At the ferromagnetic regime, a close correspondence is found between the lattice model and a circular hard-wall quantum dot.

In Publication **III**, the stability of the non-Abelian Pfaffian quantum Hall state in a confined geometry is studied. The Pfaffian wave function is found to be accurate description for suitable

forms of effective interaction between the electrons in the lowest or second lowest Landau level. However, as the Landau level mixing is included with the density functional method, it appears that the electron pairing in the second Landau level is superseded by a region of spin-droplet formation. We find indirect experimental evidence for our case but in order to clarify the issue, experiments to directly measure the spin and charge densities are proposed.

In Publication **IV**, the effects of thickness on the electron interaction and the ensuing effects to the quantum dot ground states are examined. The phase diagram is calculated, and it is found that the magic number sequence changes with the thickness embodying change in the symmetry of the corresponding Wigner molecule. We propose a set of trial wave functions that capture the physics after the transition has taken place.

Publication **V** investigates a quantum Hall droplet tunably coupled to a surrounding quantum ring. The ground-state phase diagram is calculated as a function of the position of the barrier, and the division of the angular momentum between the inner and outer systems is studied. Furthermore, the effects of compression to the magic angular momentum sequences and the edge tunneling exponent are demonstrated.

In Publication **VI**, extended quantum rings with tunable confiment potentials are studied. Results indicate that the system exhibits regimes of both antiferromagnetism and ferromagnetism, and one can switch between them by adjusting either the magnetic field or the potential.

Alternative to tuning the effective interaction, Publication **VII** studies how the confinement potential could be optimized to drive the ground-state wave function towards a sought-after form. A notable increase in the overlap is achieved by optimal adjustments.

Publication **VIII** introduces the method of density matrix functional theory for quantum Hall systems. The method performs remarkably well for a wide range of system sizes and beyond the system sizes reachable by the exact diagonalization, and thus it appears a promising method to try in other nanostructures as well.

Bibliography

[1] A. B. Fowler, F. F. Fang, W. E. Howard, and P. J. Stiles, *Magneto-oscillatory conductance in silicon surfaces*, Phys. Rev. Lett. **16**, 901 (1966).

[2] R. Dingle, W. Wiegmann, and C. H. Henry, *Quantum states of confined carriers in very thin Al_x Ga_{1-x}As-GaAs-Al_xGa_{1-x}As heterostructures*, Phys. Rev. Lett. **33**, 827 (1974).

[3] *Proceedings of the International Conference on Electronic Properties of Two-Dimensional Systems*, Surf. Sci. **58**, (1976), Physica E **42**, (2010).

[4] J. H. Davies, *The Physics of Low-Dimensional Semiconductors: An Introduction*, Cambridge University Press, Cambridge (1998).

[5] H. L. Stormer, D. C. Tsui, and A. C. Gossard, *The fractional quantum Hall effect*, Rev. Mod. Phys. **71**, S298 (1999).

[6] L. P. Kouwenhoven and C. M. Marcus, *Quantum dots*, Physics World **11**, 35 (1998).

[7] L. Jacak, P. Hawrylak, and A. Wójs, *Quantum Dots*, Springer, Berlin (1998).

[8] M. A. Reed, R. T. Bate, K. Bradshaw, W. M. Duncan, W. R. Frensley, J. W. Lee, and H. D. Shih, *Spatial quantization in GaAsAlGaAs multiple quantum dots*, J. Vac. Sci. Technol. B **4**, 358 (1986).

[9] D. Loss and D. P. DiVincenzo, *Quantum computation with quantum dots*, Phys. Rev. A **57**, 120 (1998).

[10] S. Coe-Sullivan, *Quantum dot developments*, Nature Photonics **3**, 315 (2009).

[11] Y. Arakawa and H. Sakaki, *Multidimensional quantum well laser and temperature dependence of its threshold current*, Appl. Phys. Lett. **40**, 939 (1982).

[12] R. J. Ellingson, M. Beard, J. Johnson, P.Yu, O.I. Micic, A. J. Nozik, A. Shaebev, and A. L. Efros, *Highly efficient multiple exciton generation in colloidal PbSe and PbS quantum dots*, Nano Letters **5**, 865 (2005).

[13] M. A. Walling, J. A. Novak, and J. R. E. Shepard, *Quantum dots for live cell and in vivo imaging*, Int. J. Mol. Sci. **10**, 441 (2009).

[14] E. Tölö, *Electrons on a rectangle*, Special Assignment, Helsinki University of Technology, Espoo (2007).

[15] V. Fock, *Bemerkung zur Quantelung des harmonischen Oszillators im Magnetfeld*, Zeitschrift für Physik **47**, 446 (1928).

[16] C. G. Darwin, *The diamagnetism of the free electron*, Proc. Cambridge Phil. Soc. **27**, 86 (1930).

[17] J. Suorsa, *Phase vortices and many-body states in the lowest Landau level*, M. Sc. thesis, Helsinki University of Technology, Espoo (2006).

[18] W. Y. Ruan, Y. Y. Liu, C. G. Bao, and Z. Q. Zhang, *Origin of magic angular momenta in few-electron quantum dots*, Phys. Rev. B **51**, 7942 (1995).

[19] H. Saarikoski, A. Harju, M. J. Puska, and R. M. Nieminen, *Vortex clusters in quantum dots*, Phys. Rev. Lett. **93**, 166802 (2004).

[20] M. B. Tavernier, E. Anisimovas, and F. M. Peeters, *Correlation between electrons and vortices in quantum dots*, Phys. Rev. B **70**, 155321 (2004).

[21] T. Stopa, B. Szafran, M. B. Tavernier, and F. M. Peeters, *Dependence of vortex structure in quantum dots on the range of the inter-electron interaction*, Phys. Rev. B **73**, 075315 (2006).

[22] S. He, F. C. Zhang, X. C. Xie, and S. Das Sarma, *Destruction of fractional quantum Hall effect in thick systems*, Phys. Rev. B **42**, 11376 (1990).

[23] K. von Klitzing, *25 years of quantum Hall effect (QHE), A personal view on the discovery, physics and applications of this quantum effect*, Poincaré Seminar, Paris (2004).

[24] K. von Klitzing, G. Dorda, and M. Pepper, *New method for high-accuracy determination of the fine-structure constant based on quantized Hall resistance*, Phys. Rev. Lett. **45**, 494 (1980).

[25] K. von Klitzing, *The quantized Hall effect*, Nobel Lecture, Stockholm (1985).

[26] Z. Wang and S. Xiong, *Electron-electron interactions, quantum Coulomb gap, and dynamical scaling near integer quantum Hall transitions*, Phys. Rev. B **65**, 195316 (2002).

[27] W. Pan, J.-S. Xia, V. Shvarts, D. E. Adams, H. L. Stormer, D. C. Tsui, L. N. Pfeiffer, K. W. Baldwin, and K. W. West, *Exact quantization of the even-denominator fractional quantum Hall state at $\nu = 5/2$ Landau level filling factor*, Phys. Rev. Lett. **85**, 3530 (1999).

[28] D. C. Tsui, H. L. Stormer, and A. C. Gossard, *Two-dimensional magnetotransport in the extreme quantum limit*, Phys. Rev. Lett. **48**, 1559 (1982).

[29] H. L. Stormer, *Nobel Lecture: The fractional quantum Hall effect*, Rev. Mod. Phys. **71**, 875 (1999).

[30] R. B. Laughlin, *Anomalous quantum Hall effect: An incompressible quantum fluid with fractionally charged excitations*, Phys. Rev. Lett. **50**, 1395 (1983).

[31] R. B. Laughlin, *Nobel Lecture: Fractional quantization*, Rev. Mod. Phys. **71**, 863 (1999).

[32] F. D. M. Haldane, *Fractional quantization of the Hall effect: A hierarchy of incompressible quantum fluid states*, Phys. Rev. Lett. **51**, 605 (1983).

[33] B. I. Halperin, *Statistics of quasiparticles and the hierarchy of fractional quantized Hall states*, Phys. Rev. Lett. **52**, 1583 (1984).

[34] J. K. Jain and T. Kawamura, *Composite fermions in quantum dots*, Europhys. Lett. **29**, 321 (1995).

[35] Z. F. Ezawa, *Quantum Hall Effects - Field Theoretical Approach and Related Topics*, World Scientific, Singapore (2000).

[36] R. H. Morf, *Transition from quantum Hall to compressible states in the second Landau level: New light on the $\nu = 5/2$ enigma*, Phys. Rev. Lett. **80**, 1505 (1998).

[37] I. P. Radu, J. B. Miller, C. M. Marcus, M. A. Kastner, L. N. Pfeiffer, and K. W. West, *Quasiparticle properties from tunneling in the $\nu = 5/2$ fractional quantum Hall state*, Science **320**, 899 (2008).

[38] G. Moore and N. Read, *Nonabelions in the fractional quantum Hall effect*, Nucl. Phys. B **360**, 362 (1991).

[39] M. Greiter, X.-G. Wen, and F. Wilczek, *On paired Hall states*, Nucl. Phys. B **374**, 567 (1992).

[40] S. S. Lee, S. Ryu, C. Nayak, and M. P. A. Fisher, *Particle-hole symmetry and the $\nu = 5/2$ quantum Hall state*, Phys. Rev. Lett. **99**, 236807 (2007).

[41] M. Levin, B. I. Halperin, and B. Rosenow, *Particle-hole symmetry and the Pfaffian state*, Phys. Rev. Lett. **99**, 236806 (2007).

[42] M. R. Peterson, K. Park, and S. Das Sarma, *Spontaneous particle-hole symmetry breaking in the $\nu = 5/2$ fractional quantum Hall effect*, Phys. Rev. Lett. **101**, 156803 (2008).

[43] X.-G. Wen, *Topological orders and edge excitations in FQH states*, Advances in Physics **44**, 405 (1995).

[44] S. M. Girvin and A. H. MacDonald, *Off-diagonal long range order, oblique confinement, and the fractional quantum Hall effect*, Phys. Rev. Lett. **58**, 1252 (1987).

[45] R. P. Feynman, *Simulating physics with computers*, Int. J. Theor. Phys. **21**, 467 (1982).

[46] D. P. DiVincenzo, *Quantum computation*, Science **270**, 255 (1995).

[47] E. Majorana, *Teoria simmetrica dell'elettrone e del positrone*, Nuovo Cimento **5**, 171 (1937).

[48] X.-G. Wen, *Topological order and edge structure of $\nu = 1/2$ quantum Hall state*, Phys. Rev. Lett. **70**, 355 (1993).

[49] R. de-Picciotto, M. Reznikov, M. Heiblum, V. Umansky, G. Bunin, and D. Mahalu, *Direct observation of a fractional charge*, Nature **389**, 162 (1997).

[50] L. Saminadayar, D. C. Glattli, Y. Jin, and B. Etienne, *Observation of the e/3 fractionally charged Laughlin quasiparticle*, Phys. Rev. Lett. **79**, 2526 (1997).

[51] M. Dolev, M. Heiblum, V. Umansky, Ady Stern, and D. Mahalu, *Observation of a quarter of an electron charge at the $\nu = 5/2$ quantum Hall state*, Nature **452**, 829 (2008).

[52] R. L. Willett, L. N.Pfeiffer, K. W. West, *Measurement of filling factor $5/2$ quasiparticle interference with observation of charge $e/4$ and $e/2$ period oscillations*, Proc. Natl. Acad. Sci. U.S.A. **106**, 8853 (2009).

[53] E. Tölö, *Quasiparticles in quantum Hall droplets*, M. Sc. thesis, Helsinki University of Technology, Espoo (2008).

[54] D. Arovas, J. R. Schriffer, and F. Wilczek, *Fractional statistics and the quantum Hall effect*, Phys. Rev. Lett. **53**, 722 (1984).

[55] J. M. Leinaas and J. Myrheim, *On the theory of identical particles*, Il Nuovo Cimento **37**, 1 (1977).

[56] F. Wilczek, *Magnetic flux, angular momentum, and statistics*, Phys. Rev. Lett. **48**, 1144 (1982).

[57] A. Yu. Kitaev, *Fault-tolerant quantum computation by anyons*, Ann. Phys. **303**, 2 (2003).

[58] C. Nayak, S. H. Simon, A. Stern, M. Freedman, and S. Das Sarma, *Non-Abelian anyons and topological quantum computation*, Rev. Mod. Phys. **80**, 1083 (2008).

[59] F. E. Camino, Wei Zhou, and V. J. Goldman, *Realization of a Laughlin quasiparticle interferometer: Observation of fractional statistics*, Phys. Rev. B **72**, 075342 (2005).

[60] W. Bishara, P. Bonderson, C. Nayak, K. Shtengel, and J. K. Slingerland, *Interferometric signature of non-Abelian anyons*, Phys. Rev. B **80**, 155303 (2009).

[61] B. I. Halperin, *Quantized Hall conductance, current-carrying edge states, and the existence of extended states in a two-dimensional disordered potential*, Phys. Rev. B **25**, 2185 (1982).

[62] X.-G. Wen, *Theory of the edge states in fractional quantum Hall effects*, Int. J. Mod. Phys. **B6**, 1711 (1992).

[63] M. Grayson, *Electron correlations at the fractional quantum Hall edge*, Solid State Comm. **140**, 66 (2006).

[64] A. M. Chang, *Chiral Luttinger liquids at the fractional quantum Hall edge*, Rev. Mod. Phys. **75**, 1449 (2003).

[65] X. Wan, F. Evers, and E. H. Rezayi, *Universality of the edge-tunneling exponent of fractional quantum Hall liquids*, Phys. Rev. Lett. **94**, 166804 (2005).

[66] W. Kohn, *Nobel Lecture: Electronic structure of matter – wave functions and density functionals*, Rev. Mod. Phys. **71**, 1253 (1999).

[67] J. A. Pople, *Nobel Lecture: Quantum chemical models*, Rev. Mod. Phys. **71**, 1267 (1999).

[68] E. Tölö, *Numerical calculation of configuration-interaction matrix elements*, Special Assignment, Helsinki University of Technology, Espoo (2006).

[69] E. V. Tsiper, *Analytic Coulomb matrix elements in the lowest Landau level in disk geometry*, J. Math. Phys. **43**, 1664 (2002).

[70] J. M. Thijssen, *Computational Physics*, Cambridge University Press, Cambridge (1999).

[71] E. Anderson, Z. Bai, C. Bischof, S. Blackford, J. Demmel, J. Dongarra, J. Du Croz, A. Greenbaum, S. Hammarling, A. McKenney, and D. Sorensen, *LAPACK Users' Guide 3rd ed.*, Society for Industrial and Applied Mathematics, Philadelphia (1999).

[72] R. B. Laughlin, *Quantized motion of three two-dimensional electrons in a strong magnetic field*, Phys. Rev. B **27**, 3383 (1983).

[73] D. Yoshioka, B. I. Halperin, and P. A. Lee, *Ground state of two-dimensional electrons in strong magnetic fields and* $1/3$ *quantized Hall effect*, Phys. Rev. Lett. **50**, 1219 (1983).

[74] M. R. Peterson, Th. Jolicoeur, and S. Das Sarma, *Finite-layer thickness stabilizes the Pfaffian state for the* $5/2$ *fractional quantum Hall effect: Wave function overlap and topological degeneracy*, Phys. Rev. Lett. **101**, 016807 (2008).

[75] A. Wójs, *Transition from Abelian to non-Abelian quantum liquids in the second Landau level*, Phys. Rev. B **80**, 041104(R) (2009).

[76] A. Wójs and J. J. Quinn, *Landau level mixing in the* $\nu = 5/2$ *fractional quantum Hall state*, Phys. Rev. B **74**, 235319 (2006).

[77] A. E. Feiguin, E. Rezayi, C. Nayak, and S. Das Sarma, *Density matrix renormalization group study of incompressible fractional quantum Hall states*, Phys. Rev. Lett. **100**, 166803 (2008).

[78] P. Hohenberg and W. Kohn, *Inhomogeneous electron gas*, Phys. Rev. **136**, B864 (1964).

[79] W. Kohn and L. J. Sham, *Self-consistent equations including exchange and correlation effects*, Phys. Rev., A1133 (1965).

[80] R. Stowasser and R. Hoffmann, *What do the Kohn-Sham orbitals and eigenvalues mean?*, J. Am. Chem. Soc. **121**, 3414 (1999).

[81] C. Attaccalite, S. Moroni, P. Gori-Giorgi, and G. B. Bachelet, *Correlation energy and spin polarization in the 2D electron gas*, Phys. Rev. Lett. **88**, 256601 (2002).

[82] S. M. Reimann and M. Manninen, *Electronic structure of quantum dots*, Rev. Mod. Phys. **74**, 1283 (2002).

[83] H. Saarikoski, *Density-functional approaches to interacting electrons in quantum dots*, Ph. D. thesis, Helsinki University of Technology, Espoo (2003).

[84] E. Räsänen, *Electronic properties of non-circular quantum dots*, Ph. D. thesis, Helsinki University of Technology, Espoo (2004).

[85] A. J. Coleman, *Reduced density matrices - then and now*, Int. J. Quantum Chem. **85**, 196 (2001).

[86] K. Husimi, *Some formal properties of the density matrix*, Proc. Phys. Math. Soc. Japan **22**, 264 (1940).

[87] A. E. Rothman and D. A. Mazziotti, *Variational reduced-density-matrix theory applied to the electronic structure of few-electron quantum dots*, Phys. Rev. A **78**, 032510 (2008).

[88] T. L. Gilbert, *Hohenberg-Kohn theorem for nonlocal external potentials*, Phys. Rev. B **12**, 2111 (1975).

[89] N. N. Lathiotakis, N. Helbig, and E. K. U. Gross, *Performance of one-body reduced density-matrix functionals for the homogeneous electron gas*, Phys. Rev. B **75**, 195120 (2007).

[90] N. N. Lathiotakis, N. Helbig, A. Zacarias, and E. K. U. Gross, *A functional of the one-body-reduced density matrix derived from the homogeneous electron gas: Performance for finite systems*, J. Chem. Phys. **130**, 064109 (2009).

[91] N. N. Lathiotakis and M. A. L. Marques, *Benchmark calculations for reduced density-matrix functional theory*, J. Chem. Phys. **128**, 184103 (2008).

[92] M. Piris, J. M. Matxain, X. Lopez, and J. M. Ugalde, *Communications: Accurate description of atoms and molecules by natural orbital functional theory*, J. Chem. Phys. **132**, 031103 (2010).

[93] W. M. Foulkes, L. Mitas, R. J. Needs, and G. Rajagopal, *Quantum Monte Carlo simulations of solids*, Rev. Mod. Phys. **73**, 33 (2001).

[94] A. Harju, *Variational Monte Carlo for interacting electrons in quantum dots*, J. Low Temp. Phys. **40**, 181 (2005).

[95] G. Ortiz, D. M. Ceperley, and R. M. Martin, *New stochastic method for systems with broken time-reversal symmetry: 2D fermions in a magnetic field*, Phys. Rev. Lett. **73**, 2777 (1993).

[96] E. Tölö, *Variational Monte Carlo on a quantum wire*, Special Assignment, Helsinki University of Technology, Espoo (2007).

[97] A. D. Güçlü, G. S. Jeon, and C. J. Umrigar, and J. K. Jain, *Quantum Monte Carlo study of composite fermions in quantum dots: The effect of Landau-level mixing*, Phys. Rev. B **72**, 205327 (2005).

[98] Y. Tserkovnyak and S. H. Simon, *Monte Carlo evaluation of non-Abelian statistics*, Phys. Rev. Lett. **90**, 016802 (2003).

[99] I. Dimov, B. I. Halperin, and C. Nayak, *Spin order in paired quantum Hall states*, Phys. Rev. Lett. **100**, 126804 (2008).